Journal of Advanced Research 44 (2023) 213–225

Contents lists available at ScienceDirect

Journal of Advanced Research

journal homepage: www.elsevier.com/locate/jare

Original Article

Lung specific homing of diphenyleneiodonium chloride improves pulmonary fibrosis by inhibiting macrophage M2 metabolic program

Huirui Wang [a], Yinghui Gao [a], Li Wang [b], Yang Yu [c], Jiaozhen Zhang [a], Chunyu Liu [a], Yaxin Song [a], Haochuan Xu [d], Jingcheng Wang [a], Hongxiang Lou [a,*], Ting Dong [a,*]

[a] Department of Natural Product Chemistry, Key Laboratory of Chemical Biology (Ministry of Education), School of Pharmaceutical Sciences, Cheeloo College of Medicine, Shandong University, Jinan, China
[b] Respiratory Medicines, The Affiliated Hospital of Yanan University, Yan'an, Shaanxi, China
[c] Advanced Medical Research Institute, Cheeloo College of Medicine, Shandong University, Jinan, China
[d] Peking University Health Science Center, Beijing, China

HIGHLIGHTS

- Pulmonary macrophages of PF at late stage exhibited predominantly the M2 phenotype with correlated metabolism.
- DPI inhibits M2-like macrophage polarization in vitro.
- IMS and chemical proteomics analysis showed that DPI specifically is homing to pulmonary macrophages *in vivo*.
- DPI improves bleomycin-induced pulmonary fibrosis in mice.
- DPI inhibits bleomycin-induced M2 polarization of macrophages *in vivo*.

GRAPHICAL ABSTRACT

Imaging mass spectrometry (IMS) and chemical proteomics approaches reveal DPI specifically is homing to pulmonary macrophages, resulting in M2 macrophages inhibition, and concomitant improvement in fibrosis mice.

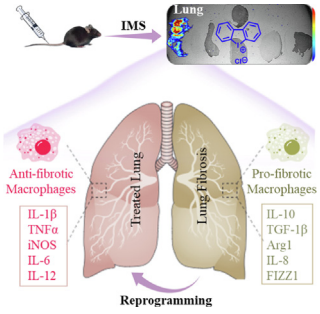

ARTICLE INFO

Article history:
Received 24 January 2022
Revised 20 April 2022
Accepted 22 April 2022
Available online 29 April 2022

Keywords:
Lung fibrosis
Diphenyleneiodonium chloride
Imaging mass spectrometry
Chemical proteomics

ABSTRACT

Introduction: Pulmonary fibrosis (PF) is a fatal disease with a variable and unpredictable course. Effective clinical treatment for PF remains a challenge due to low drug accumulation in lungs and imbalanced polarization of pro/anti-fibrotic macrophages.
Objectives: To identify the alteration of immunometabolism in the pulmonary macrophages and investigate the feasibility of specific inhibition of M2 activation of macrophages as an effective anti-PF strategy *in vivo*.
Methods: The high-content screening system was used to select lung-specific homing compounds that can modulate macrophage polarization. Imaging mass spectrometry (IMS) conjugated with chemical proteomics approach was conducted to explore the cells and proteins targeted by diphenyleneiodonium chloride (DPI). A bleomycin-induced fibrotic mouse model was established to examine the *in vivo* effect of DPI.
Results: Pulmonary macrophages of PF at late stage exhibited predominantly the M2 phenotype with decreased glycolysis metabolism. DPI was demonstrated to inhibit profibrotic activation of macrophages in the preliminary screening. Notably, IMS conjugated with chemical proteomics approach revealed DPI specifically targeted pulmonary macrophages, leading to the efficient protection from bleomycin-induced

Peer review under responsibility of Cairo University.
* Corresponding authors.
E-mail addresses: louhongxiang@sdu.edu.cn (H. Lou), tingdong2021@sdu.edu.cn (T. Dong).

https://doi.org/10.1016/j.jare.2022.04.012

pulmonary fibrosis in mice. Mechanistically, DPI upregulated glycolysis and suppressed M2 programming in fibrosis mice, thus resulting in pro-fibrotic cytokine inhibition, hydroxyproline biosynthesis, and collagen deposition, with a concomitant increase in alveolar airspaces.
Conclusions: DPI mediated glycolysis in lung and accordingly suppressed M2 programming, resulting in improved lung fibrosis.

Introduction

The treatment of lung diseases, particularly lung fibrosis, is one of the most challenging problems in clinical practice. One reason is the low efficiency of the conventional drug delivery systems, which results in low drug exposure to lungs. Moreover, unspecific drug distribution also causes clinical toxicity and has been a major bottleneck in the translation of potent drug candidates [1–2]. Next-generation drug delivery technologies, such as nanoparticles (e.g., liposomes) [3–4], conjugates of drugs, and affinity moieties (e.g., antibodies) [2], have overcome the limitations over traditional drug delivery systems by enhancing therapeutic selectivity and function, but have also introduced new delivery challenges. A particular challenge to deliver drugs to lungs is that the respiratory tract has evolved defense mechanisms by inactivating or removing the inhaled drugs out of the lungs once they have been deposited. Apart from these immunological, chemical, and mechanical barriers, poor inhaler technique and non-adherence to treatment also detrimentally affect pulmonary drug delivery [5]. Therefore, the discovery of novel lung-specific homing therapeutic agents not only increases drug accumulation, improves drug efficacy, and reduces drug toxicity, but also has promising benefits in the treatment of pulmonary fibrosis (PF).

PF is a common interstitial lung disease, while a lack of effective treatment leads to significant decreases in the survival rates and quality of life of PF patients [6–8]. PF is manifested by excessive extracellular matrix (ECM) deposition and fibroblast proliferation, thus resulting in impaired static lung compliance, disruption of gas exchange, and eventually, deaths from respiratory failure [9]. Pathologically, PF is likely due to a fibroproliferative and aberrant wound healing cascade driven by macrophages [8]. Pulmonary macrophages constitute approximately 70% of the immune cells in the lung environment, and are referred to as the critical sentinels of lung homeostasis by exhibiting various biological functions such as cellular senescence, collagen synthesis, host defense, epithelial integrity, and mucin production, which determines the pathological characteristics of fibrotic tissues [10–11]. Notably, pulmonary macrophage populations are heterogeneous and display remarkable plasticity, making them able to be functionally polarized in response to microenvironmental cues. Despite this diversity, they have been classified into two distinct macrophage activation states, namely, classical activation (M1 macrophages) and alternative activation (M2 macrophages), in which the latter is responsible for the pathogenesis of PF [12]. Specifically, in the context of PF, M1/M2 paradigm is dynamic and relies on different disease stages. In the early inflammatory stage, the resident alveolar macrophages (AMs) shift toward the M1 phenotype upon pathogen recognition, thus releasing various inflammatory cytokines (e.g., ROS, MCP-1, MIP-2, IL-1β, IL-6, and TNF-α), and ultimately leading to lung tissue destruction [13]. Following the late fibrotic stage, some pathogenic factors are eliminated. M1-type AMs then shift to the M2 phenotype in the presence of driving factors and induce a broad array of pro-fibrotic cytokines (e.g., TGF-β, IL-4, IL-10, and IL-13), which are involved in abnormal wound healing processes during fibrosis [14–16]. This finding was supported by clinical studies showing that patients with radiation-induced PF had elevated M1 marker in the early stage, while increased M2 marker in the fibrotic stage [10,17]. Collectively, these studies indicate that M1 macrophages prevent fibrotic response while M2 macrophages play an opposite fibrogenesis role. Hence, targeting M2 macrophage activation can serve as a potential treatment for PF [18–19]. Pirfenidone, an FDA-approved drug for PF treatment, exerts its anti-fibrotic effect partially by inhibiting M2 macrophage polarization [10,20]. Therefore, modulating the macrophage phenotype from M2 to M1 state may be a promising strategy for PF treatment.

Recent studies of the macrophage cell metabolism have focused on the close association between the polarization and metabolic state of the macrophages, as validated by the obvious metabolic state differences between M1 and M2 macrophages [21]. Pro-inflammatory macrophages (M1) are predominantly dependent on glycolysis by impairing the tricarboxylic acid (TCA) cycle and suppressing oxidative phosphorylation (OXPHOS), while anti-inflammatory macrophages (M2) rely on mitochondrial OXPHOS together with reduced glycolysis. Moreover, some nutrients, such as FAs, vitamins, and iron molecules, are involved in macrophage polarization. Collectively, macrophage polarization requires the coordination and fine-tuning of all metabolic changes [22–23]. Interfering these processes can inhibit the functional polarization of macrophages, leading to macrophage repolarization. For example, the increased expression of glucose transporter 1 (GLUT-1) improves glycolysis and metabolites in the pentose phosphate pathway, reduces oxygen consumption, and enhances M1 polarization [24]. In contrast, a loss of pyruvate dehydrogenase kinase-1-a glycolysis regulatory enzyme activity can inhibit M1 polarization and improve M2 differentiation by enhancing mitochondrial respiration [25]. These results imply that tissue-specific glucose uptake and metabolism are crucial for the polarization of macrophages into a pro-inflammatory M1 phenotype. Thus, regulating the metabolic switch between OXPHOS and glycolysis can be a good way to reprogram macrophage polarization and the corresponding immune functions. Enlightened by this, we have identified a total of 10 potential candidate compounds that reprogram M2-like phenotype to M1 in human macrophages [26]. In particular, DPI exhibited the most potent activity to reprogram pulmonary macrophages among all the candidate compounds; thus, it was selected in this study. Notably, imaging mass spectrometry (IMS) revealed its specific homing in lung macrophages, which led to its efficient protection against a bleomycin (BM)-induced PF mouse model. Mechanistically, DPI upregulated glycolysis and subsequently inhibited M2 program by decreasing the fibrosis markers (i.e., collagen and TGF-β1) and slightly increasing the anti-fibrotic markers (i.e., CD86 and iNOS), thus promoting the expansion of alveolar airspaces.

Materials and methods

Human samples

The broncho-alveolar lavage fluids (BALFs) from PF patients (n = 6) and healthy individuals (n = 7) were collected at the Affiliated Hospital of Yan'an University after obtaining written informed

consent. The samples from each group were pooled, centrifuged at 500*g* for 5 min to sediment the BALF immune cells, and then subjected to the following assay. Diagnosis of PF was performed in accordance with the American Thoracic Society (ATS)/European Respiratory Society (ERS) consensus diagnostic criteria. The study protocols were approved by the Human Assurance Committee of the Affiliated Hospital of Yan'an University.

Medium, reagents, drugs, and cytokines

Fetal bovine serum (FBS) was obtained from Life Science Production (Barnet, UK). RPMI 1640 medium containing Glutamax, sodium pyruvate, non-essential amino acids, and penicillin/streptomycin were supplied by Gibco (Paisley, UK). The cytokines IFN-γ, IL-4, and M-CSF were purchased from Biolegend (CA, USA). Oligomycin (Oligo) and 2-Deoxy-D-glucose (2-DG) were obtained from CST (Cell Signaling Technology, #9996). DPI was supplied by Bidepharm (Shanghai, China). BM was purchased from Mackin (Shanghai, China). TGF-β1 (ab215715), fibronectin (ab2413) and α-SMA (ab32575) were obtained from Abcam (CA, USA). CD86 (ab242142) and CD206 monoclonal antibody (MR5D3) were purchased from Themo Fisher (USA). EasySep™ Mouse F4/80 Positive Selection Kit was purchased from STEMCELL (#100-0659).

Cell culture and macrophage polarization

HEPF cells were cultured in DMEM supplemented with 10% (v/v) FBS (Gibco, 10099-141), penicillin (100 units/mL) and streptomycin (100 mg/ml), and maintained in a humidified 5% CO_2 incubator at 37℃. BMDMs were obtained from mice as described previously [26]. To induce bone marrow–derived macrophages (BMDMs) polarization, M1 macrophages were treated with lipopolysaccharide (LPS, 100 ng/mL) and IFN-γ (10 ng/mL) for 12 h, while M2 macrophages were exposed to 20 ng/mL IL-4 for 24 h, and then treated DPI at different concentrations, the detail information was according to a previous method [27].

Hydroxyproline assay

The levels of collagen in lung homogenates were assessed using a Hydroxyproline Assay Kit (Colorimetric, ab222941). The assay was performed in accordance with the kit's protocol.

Mouse model

PF mouse model was constructed via intratracheal instillation of 5 mg/kg BM hydrochloride. After exposure to BM for 10 days, mice were routinely examined by micro-computed tomography (micro-CT). Mice with a fibrotic lesion were randomly assigned to three experimental groups (n = 6 per group), and subjected to treatment twice per week, total 2 weeks. The mice were treated with DPI-1(0.5 mg/kg) or DPI-2 (1 mg/kg) through tail vein injection, starting on days 10, 13, 16, and 19; while those received the same amount of saline via tail vein injection were used as controls. All mice were euthanized at 28 days after BM exposure and subjected to further analyses.

Histological and immunochemical analyses

For histological analysis, formalin-fixed lung tissues were embedded in paraffin, sectioned (6 μm) onto glass slides, and stained with hematoxylin-eosin for morphological examination and Masson's trichrome for determination of collagen deposits, the lung fibrosis was scored using the modified Ashcroft scale as described previously [28]. For immunohistochemical analysis, the sections were permeabilized with 0.1% Triton X-100 in 1 × PBS for 10 min, probed with the primary CD206 and CD86 antibodies, and then stained with secondary antibodies.

Macrophage isolation from BALF

BALF was obtained by perfusing PBS into the lung tissue of experimental groups and was centrifuged to isolate cells [29]. These cells were cultured in a cell culture incubator for 2 h, and then changed medium to obtain pure primary pulmonary macrophage.

Murine endothelial cell isolation

The endothelial cells were isolated from mouse lungs using PECAM-1 antibody via immunoprecipitation. The detailed protocol was described by Abcam (murine endothelial cell isolation).

Pulmonary macrophage isolation of mouse lung tissue

Enzymatic lung digestion was conducted by adding 1 mL of Collagenase to mince lung tissue, and then centrifuge at 300*g* for 10 min to obtain the cell pellets. Finally, ammonium chloride solution was added to the cell pellet. The detailed procedure was adapted from the EasySep™ Mouse F4/80 Positive Selection Kit protocol.

Slide preparation for IMS analysis

Mouse tissues (brain, heart, lung, liver, kidney, and spleen) were freshly collected and embedded in optimal cutting temperature (OCT) compound before being cut on a cryostat at 10 μm thickness. Subsequently, these slides were stored at -80 °C overnight. On the next day, the sections were transferred into a desiccator for 1 h, and then subjected to IMS detection.

IMS analysis

IMS analysis was performed using an AFADESI ion source (AFAI-MSI, Beijing Viktor, China) coupled with a Q-Orbitrap mass spectrometer (Q Exactive, Thermo Scientific, Bremen, Germany). A mixture of acetonitrile and water (4:1, v/v) was used as the spray solvent at a flow rate of 5 μL/min. The unidirectional scanning speed in the X and Y directions was 200 μm/s. The data were obtained over a *m*/*z* range of 100–600 at a mass resolution of 70,000 in positive ion mode. The specific protocol was described previously [30]. Image analysis was performed with Mass Imager 1.0 as described previously [31].

Western blotting

The cells and tissues were harvested with RIPA buffer containing PMSF protease inhibitors. An equal volume (50 μg) of protein lysates was separated through SDS-PAGE and transferred onto PVDF membranes. After blocking in 5% (w/v) skimmed milk for 1 h at room temperature, the membranes were incubated overnight with primary antibodies. The source of each primary antibody is listed in Section 2.2.

Glucose consumption rate

BALF was sampled at the end of the experiment, followed by centrifugation to collect the cell pellet. The cells were seeded in a 96-well plate containing 100 μL culture medium at a density of 2,000 cells/well. Then, 2-DG6P uptake was measured by following the Glucose Uptake Assay Kit protocol (ab136955).

A

Samples	PF(n=6)	Control(n=7)	*P* value
Age (years)	50.26	53.41	0.5217
Smoking	32.14±12.05	35.52±20.41	0.4911
BMI	22.05±1.512	23.85±0.3318	0.3047
Sex			
Female	2	3	
Male	4	4	
Forced vital capacity (FVC)	63.41±2.04	NA	
DLCO	43.01±2.71	NA	

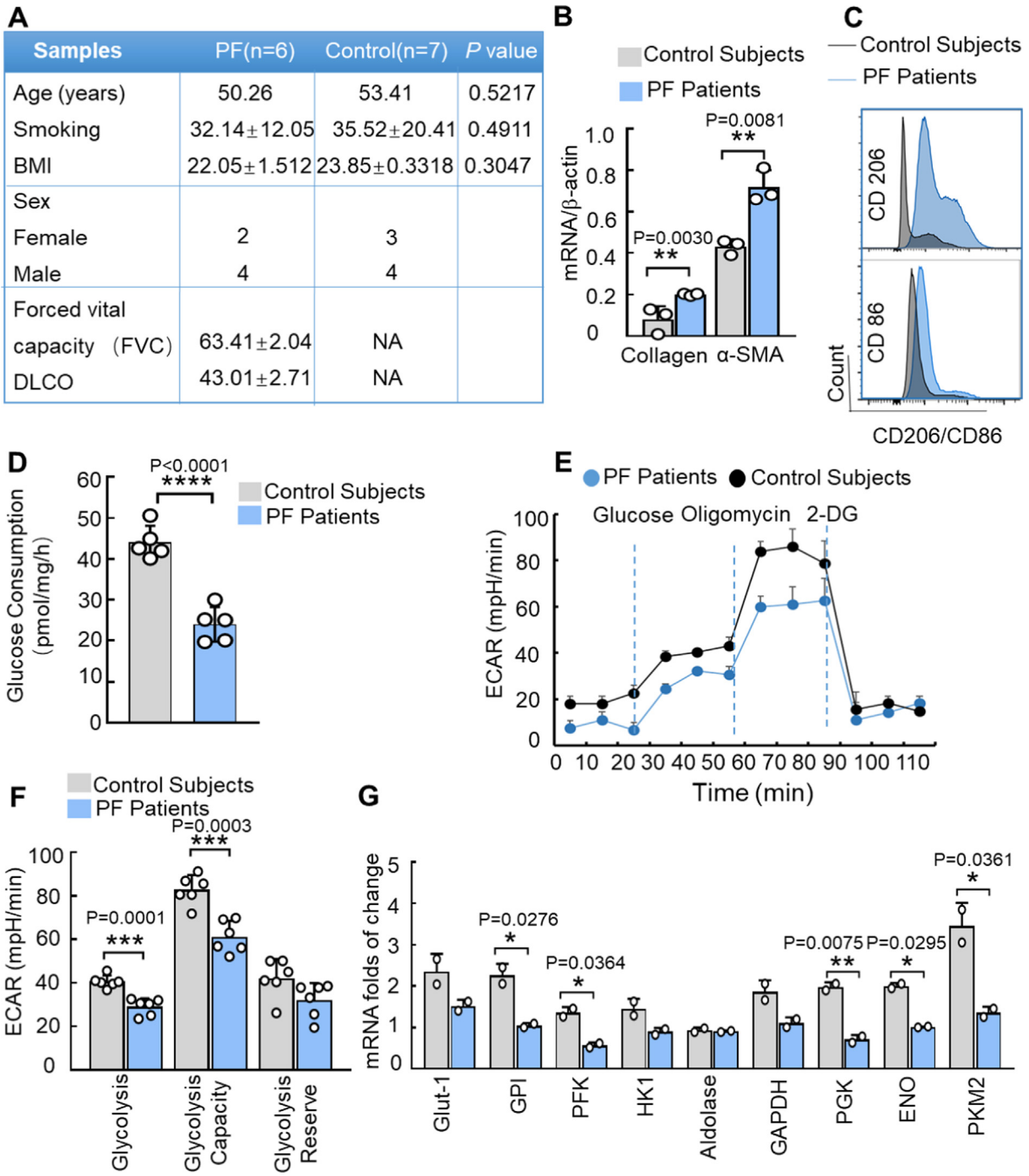

Fig. 1. PF is characterized by M2 dominant macrophages. (**A**) The characteristics of patients from which the lung specimens were obtained. (**B**) HEPF cells were seeded at the density of 5000 cells/well, after being serum-starved for 24 h. The cells were incubated with BALF for 48 h, and qPCR was performed to analyze pro-fibrotic proteins such as Collagen and α-SMA. (**C**) Flow cytometry analysis of M1 (CD86) and M2 (CD206) surface marker. (**D**) 2-DG uptake in macrophages cells (2000 cells/well) from BALF. (**E**) Extracellular acidification rate (ECAR) was measured with a glycolysis stress test. The representative kinetics were used to assess glycolysis-dependent ECAR (mpH/min) in pulmonary macrophages isolated from the PF patients by sequentially adding 10 mM glucose (Gluc), 1.25 μM oligomycin (Olig), and 50 mM 2-deoxyglucose (2-DG). (**F**) Bar graphs showing the basal ECAR levels, glycolytic capacity (GC), and glycolytic reserve (GR). (**G**) For the human samples, RNA was purified, and the mRNA level of the indicated glycolytic enzyme was measured by RT-PCR. Abbreviations: GAPDH, glyceraldehyde 3-phosphate dehydrogenase; GLUT-1, glucose transporter 1; GPI, phosphoglucose isomerase; PDK1, pyruvate dehydrogenase kinase 1; PFK, phosphofructokinase; LDH, lactate dehydrogenase; HK1, Hexokinase 1; PGK, 3-phosphoglycerate kinase; ENO, Enolase; PKM2, pyruvate kinase M2. (**H**) BALF was collected from BM-induced fibrotic mice and the glucose consumption rate was determined. (**I**) ECAR was measured with a glycolysis stress test. The representative kinetics were used to assess glycolysis-dependent ECAR (mpH/min) in pulmonary macrophages isolated from BM-induced mice by continuously adding Gluc and Olig. (**J**) Bar graphs showing the basal ECAR levels, GC and GR. (**K**) Glycolytic enzymes were examined by qPCR in BM-induced fibrotic mice.

Preparation of BALF

After euthanasia, the trachea was exposed and cannulated with 20G catheter. The lungs of mice were lavaged by instilling 0.8 mL 1X PBS (4 °C), and this process was repeated for 3–5 times. The collected BALF was centrifuged at 1500 rpm for 10 min at 4 °C, and the pellet was then resuspended with RPMI-1640 medium. Total cell count was performed using a hemocytometer or CASY1 TT Cell Counter & Analyser System (Roche Innovatis) as described previously [32].

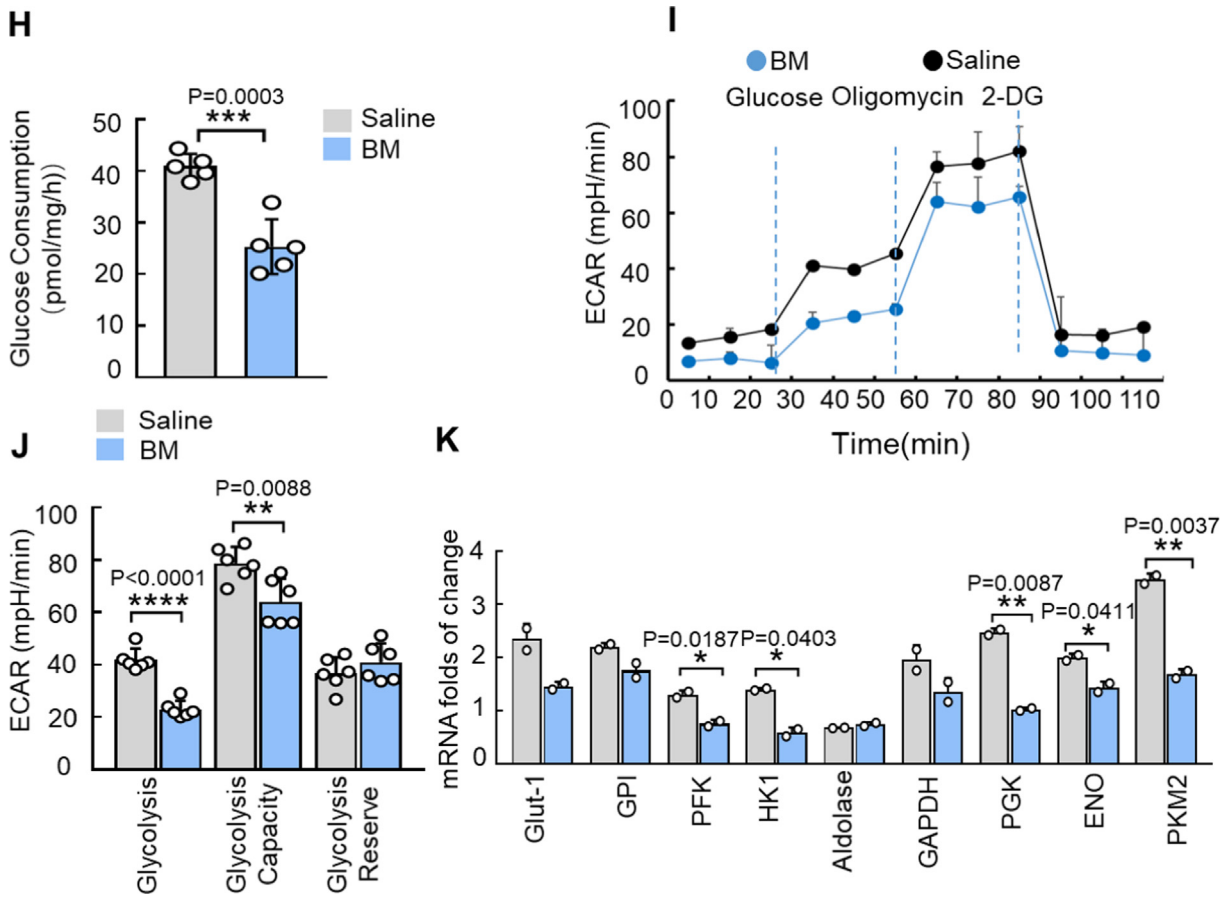

Fig. 1 (*continued*)

Ethics statement

All experiments involving animals were conducted according to the ethical policies and were approved by the Shandong University's Animal Ethics Committee (license no. 21139).

Statistical analysis

Comparison between groups was conducted using the GraphPad Prism 7 software. Differences between two groups were analyzed by Student's *t*-test with Welch's correction for unpaired data. In all cases, P-values of < 0.05 were deemed statistically significant.

Results and discussion

Pulmonary macrophages at the late-stage exhibit M2 phenotype predominantly with decreased glycolysis metabolism in PF mice

PF is a chronic progressive disease that lacks effective treatments. There is evidence indicating that lung macrophage polarization can affect the pathogenesis of PF. Particularly, M2 macrophages rather than M1 macrophages are involved in fibrotic progression by producing IL-2, IL10, and TGF-β1, which induce the differentiation of fibroblasts into myofibroblasts and exaggerate PF. In this study, BALF was sampled from 6 patients with PF, with the upregulated expression of collagen 1α1 and α-SMA (Fig. 1A-B), while 7 healthy individuals were employed as a control group. The proportions of positive cells were counted by flow cytometry using the CD86 (M1) and CD206 (M2) markers. As displayed in Fig. 1C, the expression of CD206 was remarkably higher in PF patients than in control subjects, while there was only a minor upregulation in the expression of CD86 (Fig. 1C). Macrophages usually have unique metabolic properties to better adapt to their multiple functional phenotypes, which is called metabolic reprogramming. For example, M1 macrophages can derive their energy predominantly through glycolysis, while M2 macrophages rely on OXPHOS to fuel their long-term functions. A dramatic switch in cellular metabolism is usually accompanied by their phenotypic and functional reprogramming. To investigate whether the compromised glycolysis is characterized by the presence of pro-fibrotic M2-like macrophages in PF patients, a seahorse extracellular flux analyzer was used to measure extracellular acidification rate (ECAR, a key parameter of aerobic glycolysis). As shown in Fig. 1D-F, we found that the pulmonary macrophages from PF patients had 30% decreased levels of glucose consumption and glycolytic flux compared with control subjects. To clarify the mechanisms underlying the dysregulated glycolysis of pulmonary macrophages in PF patients, the levels of cell surface glucose transporters and glycolytic enzymes were measured. It was found that the expression levels of Glut-1, GPI, PFK, HK1, Aldolase, GAPDH, PGK, ENO, and PKM2 were markedly downregulated (Fig. 1G). This metabolic remodeling matched well with the M2 dominant phenotype observed in PF patients. As for further verification, we extended the analysis from human to mouse model. Notably, metabolic reprogramming was observed in BM-induced fibrotic mice such as decreased glucose consumption (Fig. 1H), dysregulated glycolysis (Fig. 1I-J), and reduced glycolytic-related enzyme expression (Fig. 1K). These results suggest that the alternatively activated

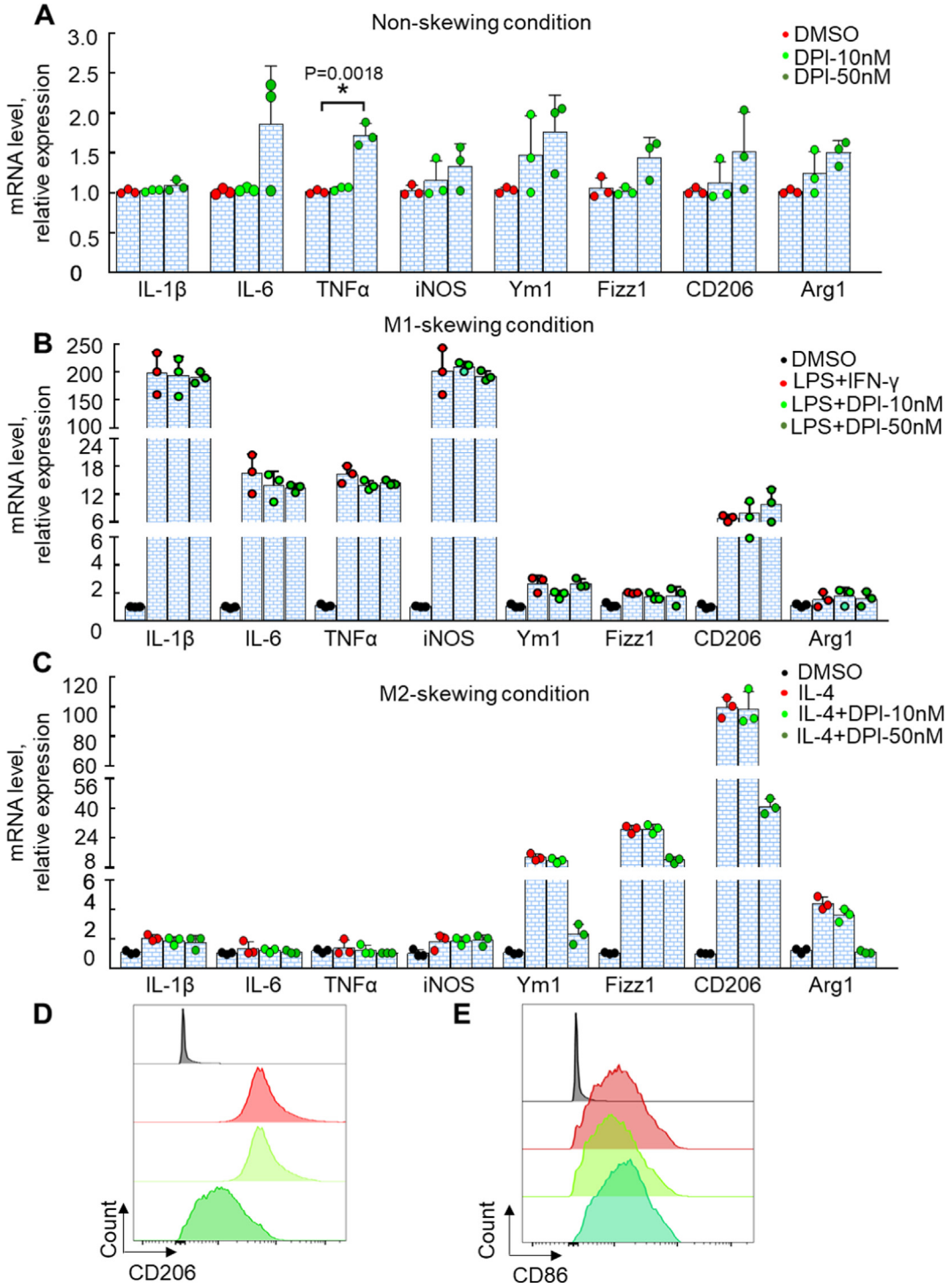

Fig. 2. DPI inhibits macrophage M2-like polarization. (**A**) The mRNA levels of Arg1, CD206, Fizz1, iNOS, IL-1β, IL-6, TNF-α, and Ym1 in non-activated BMDMs. (**B-C**) BMDMs were skewed to acquire an M1 or M2-like phenotype (see Materials and Methods) and then exposed to 0, 10, and 50 nM of DPI for 24 h. The mRNA levels of the indicated surface markers were measured by qPCR. (**D-E**) Flow cytometry analysis of M1 (CD86) and M2 (CD206) surface markers after DPI treatment.

M2 macrophages, along with decreased glycolysis, are the common pathogenic processes of PF.

DPI inhibits M2-like macrophage polarization, with no effect on M1-like polarization in vitro

Given the critical roles of dysregulated M2 macrophages in the initiation and progression of PF, we hypothesize that the reprogramming of M2 to M1 macrophages may improve PF. Our previous work has reported several chemical modulators for immune cell reprogramming [33], and DPI has the strongest suppressive effect on IL-4-triggered activation of M2-type BMDMs, as indicated by using M2 markers such as Ym1, Fizz1, CD206 and Arg1 (Supplementary Fig. 1). Moreover, 50 nM DPI could significantly inhibit M2-like macrophages, but had a minor effect on resting state or M1-like macrophages (Fig. 2A-2C). Consistently, the amount of CD206 (M2-like macrophage surface marker)-positive cells was remarkably reduced with DPI treatment (Fig. 2D), while CD86

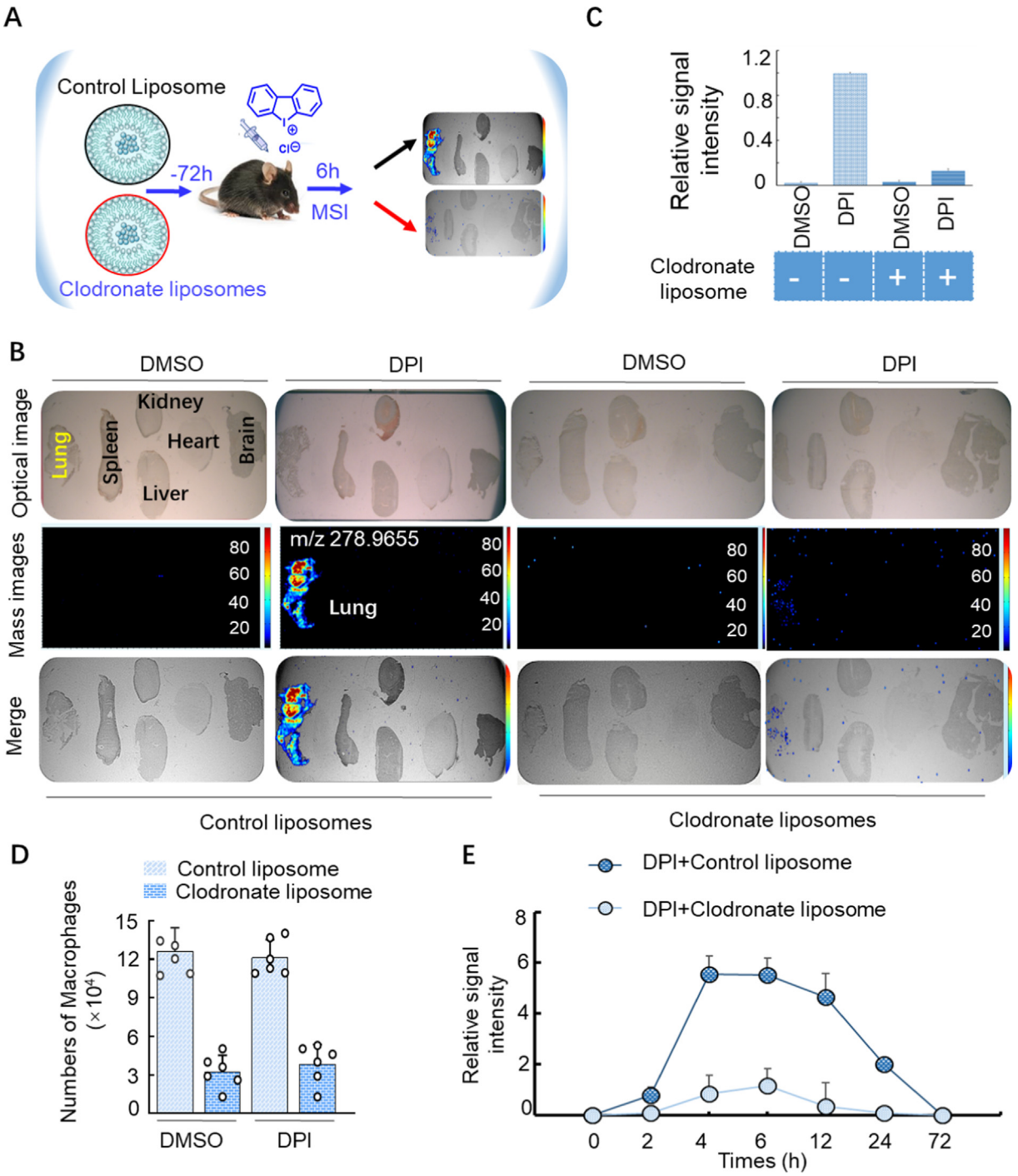

Fig. 3. Tissue homing of DPI after intravenous (IV) injection. (**A**) Optical and mass images of the $[M + H]^+$ ions at *m/z* 278.9665, corresponding to the DPI in mice. (**B-C**) Clodronate liposomes were given 72 h before DPI (1 mg/kg) injection, and the mice tissue sections were isolated for subsequent analysis. Blank liposomes were administered into the vehicle control at an equal volume. (**D**) At 6 h following DPI treatment, the BALF was sampled for the evaluation of macrophage depletion. (**E**) Concentration-time profile of DPI in lung tissues. The mice were intravenously injected with DPI (1 mg/kg) for the indicated time periods, and then analyzed by IMS.

(M1-like macrophage surface marker)-positive cells were not affected (Fig. 2E). These results suggest that DPI significantly inhibits M2-like macrophage polarization in vitro and has a minor effect on M1-like macrophages.

IMS analysis shows that DPI specifically targets pulmonary macrophages

Unwanted organ distribution of compounds not only causes safety concerns and inadequate efficacy but also determines the fate of clinical trials. Thus, we first estimated the bio-distribution of DPI before the *in vivo* test. IMS is a powerful technology used for determining the spatial distribution and quantitation of drugs and their metabolites in tissue sections without using target-specific labels or reagents. A qualitative analysis of DPI was performed on the liver, spleen, kidney, brain, heart, and lung tissues of mice. As shown in Fig. 3A, images were obtained from the tissue sections of DPI-treated mice using air-flow-assisted desorption electrospray ionization-mass spectrometry imaging (AFADESI-MSI), which was generated by extracting the ions corresponding

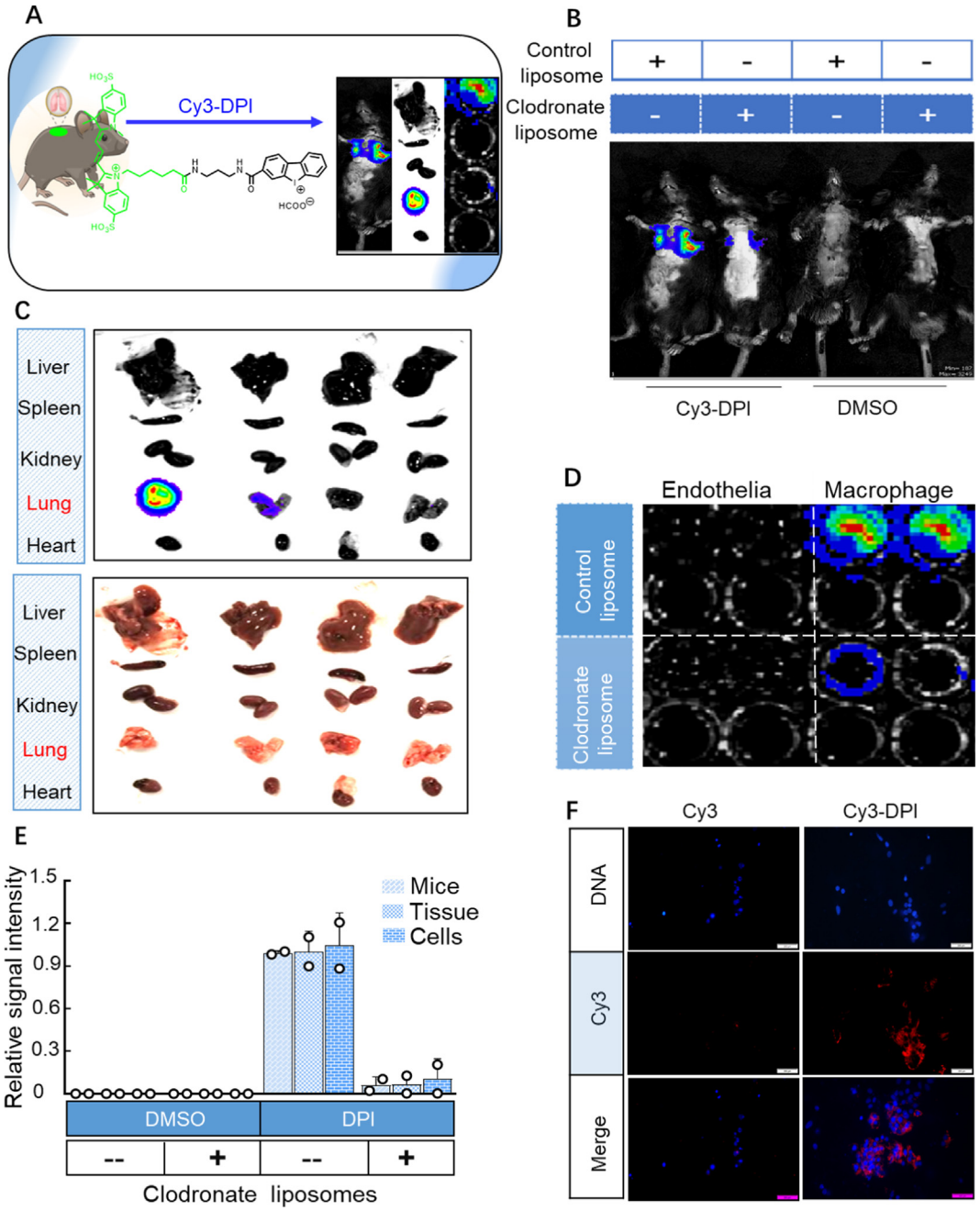

Fig. 4. Chemical proteomics study of DPI. (**A**) Schematic illustration of chemical tracking of DPI *in vivo*. (**B-D**) In vivo tracking of Cy3-DPI. The mice were given clodronate liposomes for 72 h, and then injected with or without Cy3-DPI (1 mg/kg) for 6 h, analyzed the fluorescence signals by using an in-vivo imaging instrument (PerkinElmer) in mice, tissue, or cell levels. (**E**) Quantitative analysis of the fluorescence signals in the above experimental groups. (**F**) Pre-target imaging of Cy3-DPI in living cells. The isolated pulmonary macrophages were treated with 1 μM of Cy3-DPI or Cy3 for 24 h. Before imaging on a confocal microscope, all cells were incubated with DAPI (scale bar, 200 μm).

to the drugs at *m*/*z* of 278.9665. DPI was mainly distributed in the lung rather than in the liver, heart, brain, and so on. Inspired by these findings, we further evaluated whether DPI can specifically target macrophages in fibrotic lungs. Clodronate liposome, a common macrophage-depleting agent, was applied to remove macrophages. Blank liposome or clodronate liposome was administered 72 h before DPI injection. Then, the mouse tissue section or BALF was prepared for subsequent analysis (Fig. 3B–C). Next, the intratracheal administration of clodronate liposome reduced BALF macrophages by 70% in DMSO- or DPI-treated mice (Fig. 3C–D), revealing the effective clearance of pulmonary macrophages. In the state of macrophage depletion, DPI was not detected in the lung sections (Fig. 3B), indicating that DPI specifically targets macrophages in lung tissues. Finally, the mice were treated with DPI for different periods to determine its concentration-time profiles in lung tissues, which could provide us a better dosage guidance for the *in vivo* therapy. As shown in Fig. 3E, the organ concentrations of DPI increased rapidly after its injection, peaked at 4 h, and then declined until almost disappeared on day 3. Lung accumulation of DPI was significantly higher compared with the clodronate liposome-treated group, suggesting the specific cell targeting of DPI *in vivo* (Fig. 3E).

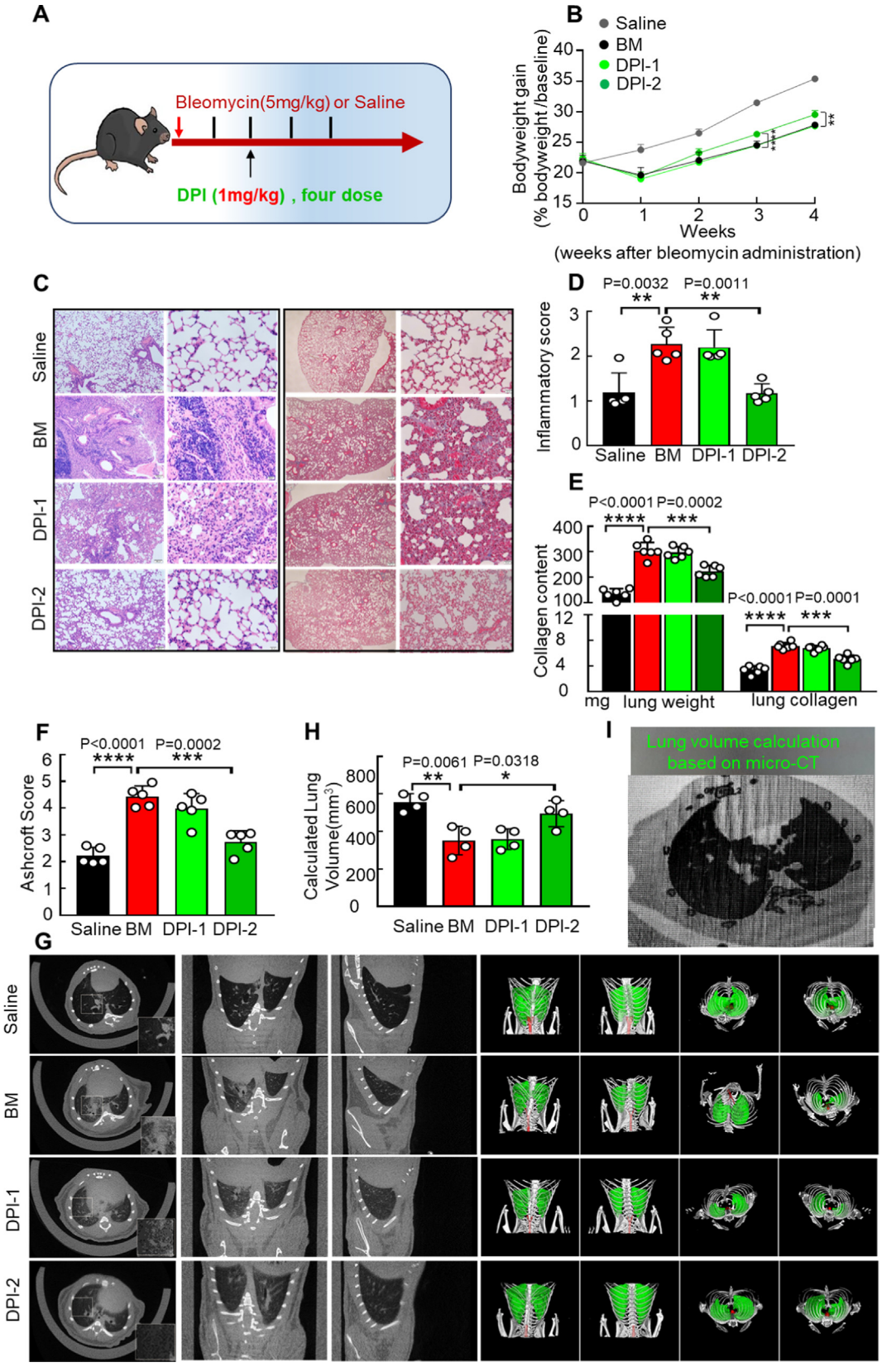
A
Bleomycin(5mg/kg) or Saline
DPI (1mg/kg) , four dose
B
Saline
BM
DPI-1
DPI-2
Bodyweight gain (% bodyweight /baseline)
Weeks
(weeks after bleomycin administration)
C
Saline
BM
DPI-1
DPI-2
D
P=0.0032
P=0.0011
Inflammatory score
Saline BM DPI-1 DPI-2
E
P<0.0001
P=0.0002
P<0.0001
P=0.0001
Collagen content
mg
lung weight
lung collagen
F
P<0.0001
P=0.0002
Ashcroft Score
Saline BM DPI-1 DPI-2
H
P=0.0061
P=0.0318
Calculated Lung Volume(mm3)
Saline BM DPI-1 DPI-2
I
Lung volume calculation based on micro-CT
G
Saline
BM
DPI-1
DPI-2

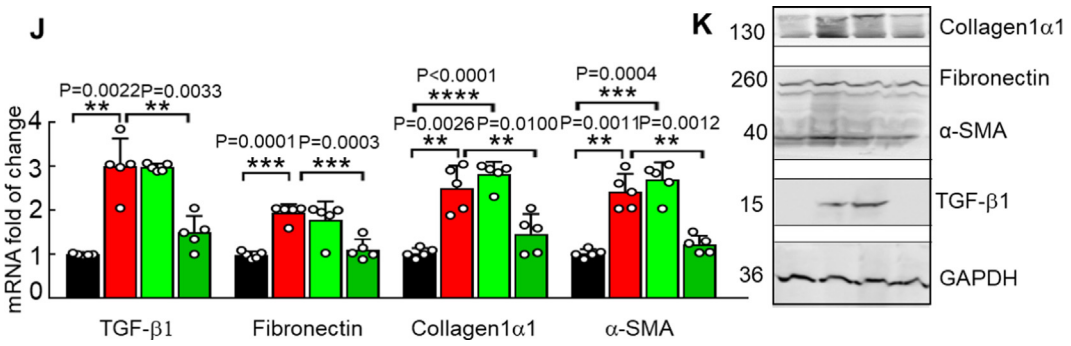

Fig. 5 (*continued*)

Chemical proteomics confirms that DPI homes to pulmonary macrophages

Apart from IMS, chemical proteomics has become an essential tool in cell biology to reveal the subcellular distribution and targeting proteins. Cy3-DPI (Supplementary scheme 1) was prepared for *in vivo* localization (Fig. 4A). Interestingly, Cy3-DPI was detected in normal mice, but not when macrophages were depleted by clodronate liposome (Fig. 4B). Further analysis of the resected tissues indicated that DPI was significantly accumulated in the lungs with minor or no absorption in other tissues, while pre-injection of clodronate liposomes into DPI-treated mice showed no fluorescence signal retained in the lungs, suggesting that DPI could target pulmonary macrophages *in vivo* (Fig. 4C). Moreover, isolation and analysis of different lung cells revealed that fluorescence signals existed in lung macrophages, but not in endothelial cells (Fig. 4-D-4E). Previous studies have shown that DPI can be used as an NADPH oxidase (NOX) inhibitor or GPR3 agonist [34]. To clarify the possible targets, fluorescence microscopy was used to pre-image the localization. The results showed that Cy3-DPI signals were mostly accumulated in the cell membrane, implying that GPR3, instead of NOX, is the possible target (Fig. 4F). Taken together, these findings demonstrate that DPI targets GPR3 in pulmonary macrophages without accumulating in other tissues.

DPI exhibits an anti-fibrotic effect on BM-induced PF mice.

Given its accumulation in pulmonary macrophages, we then sought to evaluate whether DPI can suppress PF. BM-induced PF mice were intravenously administrated with DPI or vehicle every 3 days (i.e., days 10, 13, 16 and 19), corresponding to the transitional and late phases of inflammation/fibrosis (days 7–14) and lung collagen deposition (days 14–28), respectively (Fig. 5A). Fibrosis induction resulted in a significant bodyweight loss, and DPI-2 (1 mg/kg) improved weight recovery, as pirfenidone did. (Fig. 5B, Supplementary Fig. 2). After euthanasia on day 28, BALF and lung tissue were collected from each mouse. Masson's trichrome and hematoxylin-eosin staining were conducted to evaluate extracellular collagen deposition and tissue morphology, respectively. As displayed in the histology-staining panel, the abundant levels of air sacs were found in healthy lungs, accompanied by a thin reticular basement membrane. However, BM-induced PF lungs had a significantly lower number of alveoli with a prominent extracellular matrix deposition located nearby the air sacs. Interestingly, DPI-treated PF mice had a healthy lung architecture similar to that of control mice (Fig. 5C), which was also reflected by the decreased inflammatory score (Fig. 5D), collagen deposition (Fig. 5E), and Ashcroft score (Fig. 5F). In addition to the histochemical analyses, micro-CT images of the lungs were used to predict the occurrence of pneumonia. Micro-CT is comparable to human clinical CT [35], which has been widely employed for lung studies in mouse models. Fig. 5G shows the representative micro-CT images of progressive changes in the lung functions of control and DPI-treated mice. In BM-induced fibrotic lung, there was consolidation in the alveoli, which prevented air from entering the lungs, and the entire left lung appeared as a gray area. On the contrary, DPI-treated PF mice showed fewer consolidation areas (Fig. 5G). The 3D images provide a more intuitive indication of the lung damage than 2D images and support the similar findings. As demonstrated in Fig. 5I, normal lung volume was lower in BM-induced PF mice than in control mice. However, compared with that in the BM induction group, the volume of the lungs was significantly restored in the DPI treatment group (Fig. 5H). Taken together, these data suggest that DPI-targeting fibrotic lung macrophages can inhibit all major PF hallmarks. Besides the improved morphology after DPI treatment, we also harvested lung tissues for the quantification of pro-fibrotic markers. As shown in Fig. 5J-K, DPI treatment markedly reduced the expression of TGF-β1, collagen 1α1, α-SMA, and Fibronectin in PF mice, as analyzed by qPCR or Western blot analyses. The protein levels of the fibrotic markers in DPI-treated mice were relatively similar to those in control mice, which agree well with the hypothesis that M2 macrophages are involved in the production of fibroblast-activated cytokines [10].

Fig. 5. DPI suppresses BM-induced PF in mice. (**A**) Schematic diagram of the experimental design. A single dose of BM (5.0 mg/kg) was given via intratracheal instillation on day 0. DPI-1(0.5 mg/kg) or DPI-2 (1 mg/kg) was administered every three days starting on days 10, 13, 16, and 19, and then euthanized on day 28. (**B**) Bodyweight changes in mice over time. (**C**) Hematoxylin-eosin and Masson's trichrome staining of the lung tissues (scale bar, 100 μm). (**D**) Quantification of the inflammatory score (n = 5). (**E**) Quantification of total hydroxyproline content was used as a measure to express the collagen content of each lung sample (n = 6). (**F**) Ashcroft scoring of fibrosis (n = 5). (**G**) Representative micro-CT images of the lung tissues of DPI treatment and normal mice after BM induction. Horizontal (upper row), horizontal axis (middle row) and 3D micro-CT (right image) images can be obtained four weeks after BM induction. (**H-I**) Quantification of normal lung volume was performed by using living image software, and the calculation process was recorded as a video shown in 5I. (**J**) Changes in the mRNA expression of the pro-fibrosis markers (TGF-β1, Fibronectin, collagen 1α1, and α-SMA) were evaluated by qPCR. (**K**) BALF was sampled on day 28, followed by centrifugation to separate the cell pellet. Western blot analysis was conducted to detect collagen 1α1, Fibronectin, α-SMA, and TGF-β1 protein levels. GAPDH was used as a loading control.

DPI suppresses BM-induced M2 polarization of macrophages in lung tissues, consistent with the reduced expression levels of fibrotic markers

To assess whether DPI can mediate the reprogramming of PF macrophages, BALF and lung tissues were collected from the mice in four experimental groups (Saline, BM, DPI-1, DPI-2), and the polarization and metabolic states of pulmonary macrophages were

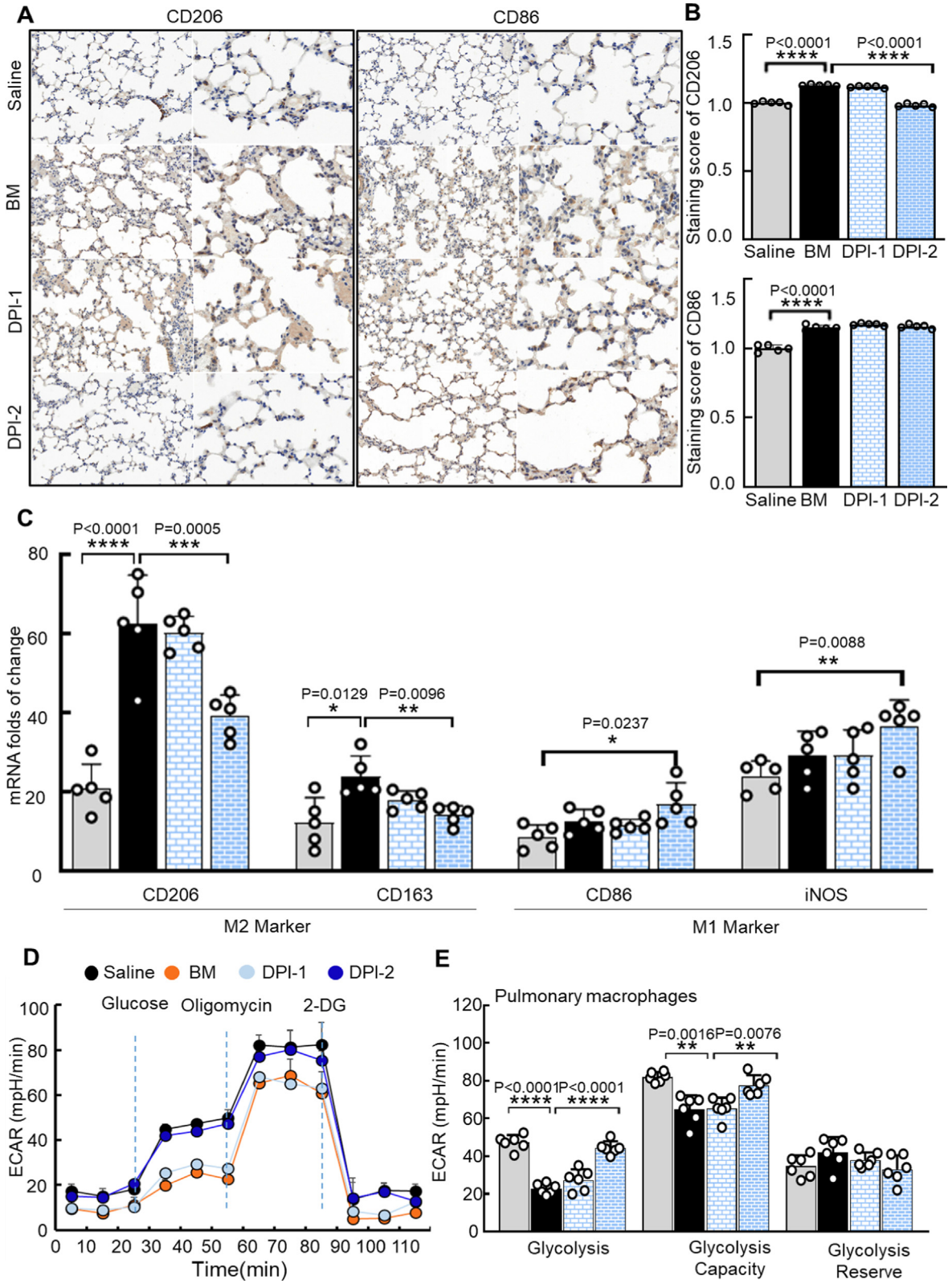

Fig. 6. DPI inhibits the expression of M2-like macrophages *in vivo*. (**A**) Immunohistochemical analysis of the surface markers CD86 (M1 macrophages typical surface marker) and CD206 (M2 macrophages typical surface marker) in the lung tissues from different experimental groups on day 28. (Scale bar: 100 μm) (**B**) Quantification of CD206 + and CD86 + IHC stained tissues of the mice (n = 5). (**C**) Changes in the mRNA levels of the macrophage markers in lung tissues after exposure to DPI or saline treatment. (**D-E**) ECAR was measured with a glycolysis stress test. The representative kinetics were used to assess glycolysis-dependent ECAR (mpH/min) pulmonary macrophages isolated from the various experimental mice by sequentially adding Gluc, Olig and 2-DG. (**E**) Bar graphs showing the basal ECAR levels, GC and GR. (**F-G**) The representative kinetics were used to assess glycolysis-dependent ECAR (mpH/min) in endothelial cells isolated from the above mice. (**G**) Bar graphs showing the basal ECAR levels, GC and GR.

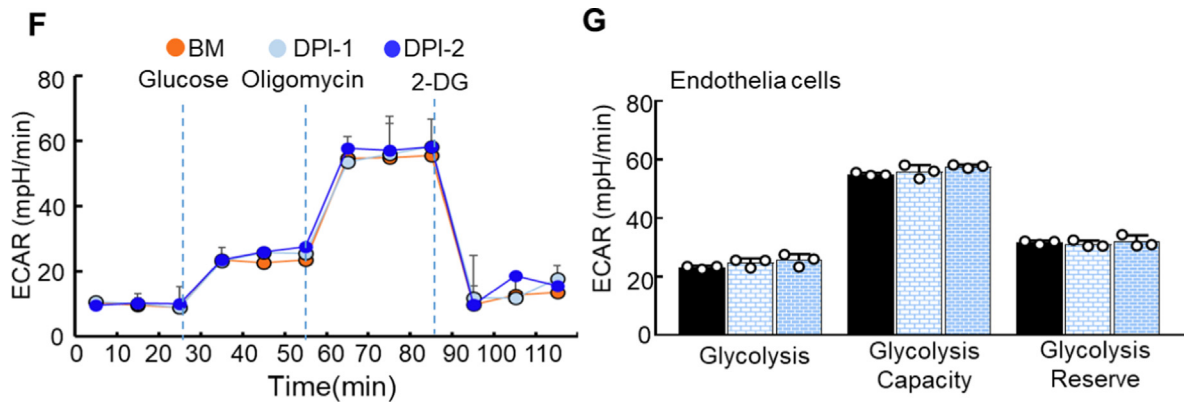

Fig. 6 (*continued*)

analyzed in parallel. First, the M2 marker (CD206) and M1 marker (CD86) were detected in the fibrotic lungs by immunofluorescence staining. As shown in Fig. 6A, CD206-positive macrophages were strongly reduced, while CD86 positive macrophages were slightly increased in DPI-2-treated lung tissues compared with the non-treated group, indicating the *in vivo* reprogramming of PF macrophages after DPI treatment (Fig. 6A-B). To confirm the immunostaining results, RT-PCR analysis was conducted on two additional macrophage markers (CD163 and iNOS), which demonstrated similar results (Fig. 6C). At the same time, we analyzed the same batch of pulmonary macrophages for their metabolic status. Consistently, DPI upregulated glycolysis to a similar level as the control groups, which was required by M1 macrophages (Fig. 6D–E). However, the effect disappeared in endothelial cells (Fig. 6F–G), confirming that DPI improves fibrotic lungs by specifically targeting pulmonary macrophages.

Conclusions

PF is manifested by the accumulation of excessive ECM in the lung parenchyma and has been associated with poor survival. The development of PF is related to the activation of α-SMA in fibroblasts, also known as myofibroblasts. Recently, pulmonary macrophages have been recognized as a key indicator for abnormal wound healing processes, due to their ability to secrete large amounts of collagen and proline as well as degrade MMPs and plasmin. Cockwell et al. indicated that infiltrating macrophages are correlated with the severity of fibrotic damage [7]. Macrophage depletion by clodronate can improve tissue injury and suppress the pro-fibrotic process [36–37]. Notably, M2-activated macrophages are directly involved in architectural remodeling and homeostasis by secreting pro-fibrotic factors (e.g., Galactin-3 and TGF-β1) [38]. The metabolic states of macrophages are closely related to their phenotypes and functions. For instance, pro-inflammatory macrophages (M1) are characterized by high glycolysis and compromised OXPHOS. Thus, we hypothesize that screening compounds that revive mitochondrial energy metabolism as indicated by OCR/ECAR, can reprogram the macrophage polarization from M2 to M1 and greatly improve lung fibrosis. In this study, we estimated the distribution ratio of M1/M2 macrophages in control subjects and PF patients. Consistent with the previously reported works, PF patients showed an increase in the levels of M2 macrophages compared with control subjects, which were relatively similar to those in BM-induced fibrosis model (Fig. 1). Our previous works have identified a series of immune modulators, including DPI, that are responsible for macrophage reprogramming. In the present study, we found that DPI might convert PF macrophages into anti-fibrotic phenotype using an in vitro system (Fig. 2). Since conventional drug delivery usually results in low efficiency and safety concerns because of unwanted organ distribution, we used IMS conjugated with chemical proteomics to map DPI directly in lung tissues and specific cell populations. As displayed in Figs. 3-4, DPI could target pulmonary macrophages, which implied its effective application in lung fibrosis-related disease. Furthermore, we evaluated the *in vivo* effect of DPI on fibrosis progression. Both micro-CT and tissue histology analyses indicated that DPI could improve lung fibrosis (Fig. 5). Finally, a mechanistic study indicated that DPI altered mitochondria metabolism and then suppressed M2 macrophages, which has important therapeutic significance to prevent ECM development during lung fibrosis progression (Fig. 6). This work not only discovered a lead compound for efficient PF therapy, but also correlated macrophage metabolism with fibrosis formation, which might deepen the understanding of fibrosis progression in the context of pulmonary macrophage metabolism regulated by this novel drug. Considering pulmonary delivery offers the potential to address unmet medical needs in lung-related disease, amounts of evidence indicates that increased proportions of the cationic lipids in nanoparticles can achieve lung-targeted delivery [39–40]. Thus, we will expect that DPI may serve as a useful head group conjugated to lipid, which would assist mRNA formulations for lung disease therapy.

Compliance with Ethics Requirements

All experiments involving animals were conducted according to the ethical policies and procedures approved by the Shandong University's Animal Ethics Committee (license no. 21139).

Declaration of Competing Interest

The authors declare that they have no known competing financial interests or personal relationships that could have appeared to influence the work reported in this paper.

Acknowledgements

We thank Yue Liu, Chan Wang and Chunyu Liu for their help with preparation of pathological section. Translational Medicine Core Facility of Shandong University for consultation and instrument availability that supported this work, Yang Yu for her help with micro-CT scanning.

Funding

This work was funded by Natural Science Fund for Excellent Young Scholars of Shandong Province of China (2022HWYQ-033),

Qilu Young Scholars Discipline Construction Funds of Shandong University (21310082163123) and National Natural Science Foundation of China (82173703).

Appendix A. Supplementary material

Supplementary data to this article can be found online at https://doi.org/10.1016/j.jare.2022.04.012.

References

[1] Ferkol T, Schraufnagel D. The global burden of respiratory disease. Ann Am Thorac Soc 2014;11(3):404–6.
[2] Patra JK, Das G, Fraceto LF, Campos EVR, Rodriguez-Torres MDP, Acosta-Torres LS, et al. Nano based drug delivery systems: recent developments and future prospects. J Nanobiotechnol 2018;16(1). doi: https://doi.org/10.1186/s12951-018-0392-8.
[3] Tiwari G, Tiwari R, Sriwastawa B, Bhati L, Pandey S, Pandey P, et al. Drug delivery systems: An updated review. Int J Pharm Investig 2012;2(1):2. doi: https://doi.org/10.4103/2230-973X.96920.
[4] Wilczewska AZ, Niemirowicz K, Markiewicz KH, Car H. Nanoparticles as drug delivery systems. Pharmacol Rep 2012;64(5):1020–37.
[5] Newman SP. Drug delivery to the lungs: challenges and opportunities. Ther Deliv 2017;8(8):647–61.
[6] Gross TJ, Hunninghake GW. Idiopathic pulmonary fibrosis. N Engl J Med 2001;345(7):517–25.
[7] King TE, Pardo A, Selman M. Idiopathic pulmonary fibrosis. Lancet 2011;378 (9807):1949–61.
[8] Wilson MS, Wynn TA. Pulmonary fibrosis: pathogenesis, etiology and regulation. Mucosal Immunol 2009;2(2):103–21.
[9] Bonnans C, Chou J, Werb Z. Remodelling the extracellular matrix in development and disease. Nat Rev Mol Cell Biol 2014;15(12):786–801.
[10] Zhang L, Wang Y, Wu G, Xiong W, Gu W, Wang CY. Macrophages: friend or foe in idiopathic pulmonary fibrosis? Respir Res 2018 Sep 6;19(1):170.
[11] Byrne AJ, Maher TM, Lloyd CM. Pulmonary Macrophages: A New Therapeutic Pathway in Fibrosing Lung Disease? Trends Mol Med 2016;22(4):303–16.
[12] Lawrence T, Natoli G. Transcriptional regulation of macrophage polarization: enabling diversity with identity. Nat Rev Immunol 2011;11(11):750–61.
[13] Delavary BM, van der Veer WM, van Egmond M, Niessen FB, Beelen RHJ. Macrophages in skin injury and repair. Immunobiology 2011;216(7):753–62.
[14] Wynn TA, Vannella KM. Macrophages in Tissue Repair, Regeneration, and Fibrosis. Immunity 2016;44(3):450–62.
[15] Wynn T, Barron L. Macrophages: master regulators of inflammation and fibrosis. Semin Liver Dis 2010;30(03):245–57.
[16] Kolb M, Margetts PJ, Anthony DC, Pitossi F, Gauldie J. Transient expression of IL-1beta induces acute lung injury and chronic repair leading to pulmonary fibrosis. J Clin Invest 2001 Jun;107(12):1529–36.
[17] Zhang H, Han G, Liu H, Chen Ji, Ji X, Zhou F, et al. The development of classically and alternatively activated macrophages has different effects on the varied stages of radiation-induced pulmonary injury in mice. J Radiat Res 2011;52 (6):717–26.
[18] Goda C, Balli D, Black M, Milewski D, Le T, Ustiyan V, et al. Loss of FOXM1 in macrophages promotes pulmonary fibrosis by activating p38 MAPK signaling pathway. PLoS Genet 2020 Apr 9;16(4):e1008692.
[19] Wang J, Xu L, Xiang Z, Ren Y, Zheng X, Zhao Q, et al. Microcystin-LR ameliorates pulmonary fibrosis via modulating CD206$^+$ M2-like macrophage polarization. Cell Death Dis 2020 Feb 19;11(2):136.
[20] Pan T, Zhou Q, Miao K, Zhang L, Wu G, Yu J, et al. Suppressing Sart1 to modulate macrophage polarization by siRNA-loaded liposomes: a promising therapeutic strategy for pulmonary fibrosis. Theranostics 2021;11 (3):1192–206.
[21] Biswas S, Mantovani A. Orchestration of metabolism by macrophages. Cell Metab 2012;15(4):432–7.
[22] Galván-Peña S, O'Neill LA. Metabolic reprograming in macrophage polarization. Front Immunol 2014 Sep;2(5):420.
[23] Liu Y, Xu R, Gu H, Zhang E, Qu J, Cao W, et al. Metabolic reprogramming in macrophage responses. Biomark Res 2021;9(1). doi: https://doi.org/10.1186/s40364-020-00251-y.
[24] Freemerman AJ, Johnson AR, Sacks GN, Milner JJ, Kirk EL, Troester MA, et al. Metabolic reprogramming of macrophages: glucose transporter 1 (GLUT1)-mediated glucose metabolism drives a proinflammatory phenotype. J Biol Chem 2014;289(11):7884–96.
[25] Min B-K, Park S, Kang H-J, Kim DW, Ham HJ, Ha C-M, et al. Pyruvate Dehydrogenase Kinase Is a Metabolic Checkpoint for Polarization of Macrophages to the M1 Phenotype. Front Immunol 2019 May;10:944.
[26] Wang Yi, Zhang L, Wu G-R, Zhou Q, Yue H, Rao L-Z, et al. MBD2 serves as a viable target against pulmonary fibrosis by inhibiting macrophage M2 program. Sci Adv 2021;7(1). doi: https://doi.org/10.1126/sciadv.abb6075.
[27] Hu G, Su Y, Kang BH, Fan Z, Dong T, Brown DR, et al. High-throughput phenotypic screen and transcriptional analysis identify new compounds and targets for macrophage reprogramming. Nat Commun 2021;12(1). doi: https://doi.org/10.1038/s41467-021-21066-x.
[28] Hübner RH, Gitter W, El Mokhtari NE, Mathiak M, Both M, Bolte H, et al. Standardized quantification of pulmonary fibrosis in histological samples. *Biotechniques* 2008;44(4):507-11, 514-7.
[29] Busch CJ, Favret J, Geirsdóttir L, Molawi K, Sieweke MH. Isolation and Long-term Cultivation of Mouse Alveolar Macrophages. Bio Protoc 2019 Jul 20;9 (14):e3302.
[30] Luo Z, Liu D, Pang X, Yang W, He J, Zhang R, et al. Whole-body spatially-resolved metabolomics method for profiling the metabolic differences of epimer drug candidates using ambient mass spectrometry imaging. Talanta 2019;202:198–206.
[31] Yang S, Banerjee S, de Freitas A, Sanders YY, Ding Q, Matalon S, et al. Participation of miR-200 in pulmonary fibrosis. Am J Pathol 2012;180 (2):484–93.
[32] Neupane AS, Willson M, Chojnacki AK, Vargas E Silva Castanheira F, Morehouse C, Carestia A, et al. Patrolling Alveolar Macrophages Conceal Bacteria from the Immune System to Maintain Homeostasis. Cell 2020;183(1). 110–125.e11.
[33] Eardley KS, Zehnder D, Quinkler M, Lepenies J, Bates RL, Savage CO, et al. The relationship between albuminuria, MCP-1/CCL2, and interstitial macrophages in chronic kidney disease. Kidney Int 2006;69(7):1189–97.
[34] Ye C, Zhang Z, Wang Z, Hua Q, Zhang Ru, Xie X. Identification of a novel small-molecule agonist for human G protein-coupled receptor 3. J Pharmacol Exp Ther 2014;349(3):437–43.
[35] Paulus MJ, Gleason SS, Kennel SJ, Hunsicker PR, Johnson DK. High resolution X-ray computed tomography: an emerging tool for small animal cancer research. Neoplasia 2000;2(1-2):62–70.
[36] Lim JH. Liver Flukes: the Malady Neglected. Korean J Radiol 2011;12(3):269. doi: https://doi.org/10.3348/kjr.2011.12.3.269.
[37] Kitamoto K, Machida Y, Uchida J, Izumi Y, Shiota M, Nakao T, et al. Effects of liposome clodronate on renal leukocyte populations and renal fibrosis in murine obstructive nephropathy. J Pharmacol Sci 2009;111(3):285–92.
[38] Vernon MA, Mylonas KJ, Hughes J. Macrophages and renal fibrosis. Semin Nephrol 2010;30(3):302–17.
[39] Cheng Q, Wei T, Farbiak L, Johnson LT, Dilliard SA, Siegwart DJ. Selective organ targeting (SORT) nanoparticles for tissue-specific mRNA delivery and CRISPR-Cas gene editing. Nat Nanotechnol 2020;15(4):313–20.
[40] Hou X, Zaks T, Langer R, Dong Y. Lipid nanoparticles for mRNA delivery. Nat Rev Mater 2021;6(12):1078–94.